Data-Driven Respiratory Gating Outperforms Device-Based Gating for Clinical ^{18}F-FDG PET/CT

Matthew D. Walker[1], Andrew J. Morgan[1], Kevin M. Bradley[2,3], and Daniel R. McGowan[1,4]

[1]Radiation Physics and Protection, Oxford University Hospitals NHS FT, Oxford, United Kingdom; [2]Department of Radiology, Churchill Hospital, Oxford, United Kingdom; [3]Wales Research and Diagnostic PET Imaging Centre, Cardiff University, Cardiff, United Kingdom; and [4]Department of Oncology, University of Oxford, Oxford, United Kingdom

A data-driven method for respiratory gating in PET has recently been commercially developed. We sought to compare the performance of the algorithm with an external, device-based system for oncologic ^{18}F-FDG PET/CT imaging. **Methods:** In total, 144 whole-body ^{18}F-FDG PET/CT examinations were acquired, with a respiratory gating waveform recorded by an external, device-based respiratory gating system. In each examination, 2 of the bed positions covering the liver and lung bases were acquired with a duration of 6 min. Quiescent-period gating retaining approximately 50% of coincidences was then able to produce images with an effective duration of 3 min for these 2 bed positions, matching the other bed positions. For each examination, 4 reconstructions were performed and compared: data-driven gating (DDG) (we use the term *DDG-retro* to distinguish that we did not use the real-time R-threshold–based application of DDG that is available within the manufacturer's product), external device-based gating (real-time position management (RPM)–gated), no gating but using only the first 3 min of data (ungated-matched), and no gating retaining all coincidences (ungated-full). Lesions in the images were quantified and image quality scored by a radiologist who was masked to the method of data processing. **Results:** Compared with the other reconstruction options, DDG-retro increased the SUV_{max} and decreased the threshold-defined lesion volume. Compared with RPM-gated, DDG-retro gave an average increase in SUV_{max} of 0.66 ± 0.1 g/mL ($n = 87$, $P < 0.0005$). Although the results from the masked image evaluation were most commonly equivalent, DDG-retro was preferred over RPM-gated in 13% of examinations, whereas the opposite occurred in just 2% of examinations. This was a significant preference for DDG-retro ($P = 0.008$, $n = 121$). Liver lesions were identified in 23 examinations. Considering this subset of data, DDG-retro was ranked superior to ungated-full in 6 of 23 (26%) cases. Gated reconstruction using the external device failed in 16% of examinations, whereas DDG-retro always provided a clinically acceptable image. **Conclusion:** In this clinical evaluation, DDG-retro provided performance superior to that of the external device-based system. For most examinations the performance was equivalent, but DDG-retro had superior performance in 13% of examinations, leading to a significant preference overall.

Key Words: respiratory gating; PET/CT; RPM; data-driven gating; FDG

J Nucl Med 2020; 61:1678–1683
DOI: 10.2967/jnumed.120.242248

Respiratory motion leads to a degradation of image quality in clinical PET/CT. The amplitude of the organ motion and deformation associated with respiration varies substantially between patients, with liver motion of 2–3 cm not uncommon (*1,2*). These amplitudes exceed the spatial resolution of modern PET scanners (*3*). The respiratory period is typically in the range 3–6 s, which is far shorter than PET acquisition durations of 2–3 min per bed position. In the absence of respiratory gating, PET images are hence blurred by the motion of many respiratory cycles. This blurring is particularly notable during imaging of the upper abdomen and lower thorax. Nevertheless, respiratory gating has yet to be adopted as a standard requirement for routine clinical ^{18}F-FDG PET/CT imaging (*3*).

There are several approaches to respiratory gating in PET (*4*). Commercially available external devices can be used to track the motion of the chest wall and thus provide a respiratory waveform that can be used for gating. Such devices have been in clinical use for several years and include a camera-based, real-time position management (RPM) system (Varian Medical Systems) and a pressure-belt–based system (AZ-733VI; Anzai Medical). An alternative approach is to extract a respiratory waveform from the PET data itself. Such a data-driven gating (DDG) approach has recently been developed and commercialized by a scanner manufacturer (GE Healthcare), offering improved workflow with reduced patient setup time. The algorithm makes use of principal component analysis to extract a respiratory waveform from the PET data. Early versions of this method were developed and evaluated by the team of Thielemans (*5–7*). The commercial version has been evaluated in phantom studies, which found it to reliably provide a respiratory waveform (*8*). The quality of the waveforms extracted by the algorithm have been assessed from clinical ^{18}F-FDG PET data, and examples of suitable and unsuitable waveforms have been published (*9*). Clinical examples have also been published (*8,10*).

In the current study, we performed a clinical evaluation of principal component analysis–based DDG for ^{18}F-FDG PET/CT, with a comparison to respiratory gating using an external device and to ungated data. Because DDG extracts a respiratory waveform from the 3-dimensional motion of the radioactivity within the internal organs (as opposed to tracking the rise and fall of the chest wall (*11*)), we hypothesized that DDG would provide images with improved mitigation of respiratory motion as compared with device-based gating using an external, camera-based tracking system (*12,13*). To our knowledge, this was the first large-scale evaluation of a DDG algorithm that is in clinical use. Büther et al. (*14*) recently evaluated a DDG algorithm developed for use with

Received Jan. 14, 2020; revision accepted Mar. 16, 2020.
For correspondence or reprints contact: Matthew D. Walker, Radiation Physics and Protection, Oxford University Hospitals NHS FT, Old Rd., Headington, Oxford, OX3 7LE, U.K.
E-mail: matthew.walker@ouh.nhs.uk
Published online Apr. 3, 2020.

continuous-bed-motion acquisition and demonstrated similar performance between DDG and device-based gating. Other DDG algorithms have been evaluated clinically but await commercial implementation (*15,16*).

MATERIALS AND METHODS

Patient Selection

The study made use of 144 whole-body ^{18}F-FDG PET/CT examinations acquired in August 2018 at the Churchill Hospital, Oxford. They represent an unbiased sample of ^{18}F-FDG PET/CT examinations as performed at the hospital, which is a regional public cancer center. The study was performed retrospectively and was approved by the Institutional Review Board and Health Research Authority (approval 19/HRA/0315); the need for written informed consent was waived.

PET/CT Acquisition Protocol

Data were acquired using a Discovery 690 or Discovery 710 PET/CT scanner (GE Healthcare) (*17*). After a minimum of 6 h of fasting, patients received ^{18}F-FDG intravenously at a dose of 4 MBq/kg of body weight. They rested for a 90-min uptake period before commencement of the PET/CT acquisition. A marker block was attached to the patient's chest, allowing for respiratory motion to be tracked by an infrared camera (RPM) that was attached at the foot of the patient couch. A scout scan was acquired, from which 2 bed positions were identified by the PET/CT technologist for application of respiratory gating. These bed positions were the 2 positions that covered the liver and the base of the lungs. A free-breathing helical CT scan was then acquired, followed by the PET scan.

The acquisition duration for the 2 bed positions with respiratory gating was set to 6 min per position. This duration was chosen such that on application of quiescent-period respiratory gating, with retention of approximately 50% of coincidences, an effective acquisition duration of 3 min per bed position was maintained. The other bed positions, for which respiratory gating was not intended, had acquisition durations set to 3 min. The PET bed-position overlap was 23%.

Respiratory Gating and Image Reconstruction

The manufacturer's Bayesian penalized-likelihood reconstruction algorithm (Q.Clear) was used, with a β-value of 400 (*18*), to create 4 PET datasets from each examination. These were reconstructed with no respiratory gating retaining all data (termed ungated-full); no respiratory gating but retaining only the first 3 min from each of the two 6-min bed positions (termed ungated-matched); quiescent-period respiratory gating (*19*) applied only to the two 6-min bed positions, with the gating signal provided by the external device (termed RPM-gated); and quiescent-period respiratory gating applied only to the two 6-min bed positions, with the gating signal extracted from the PET data using the manufacturer's algorithm (MotionFree) (termed DDG-retro). We use the term *retro* to distinguish that we did not use the real-time R-threshold based application of DDG that is available within the MotionFree product (2019 release).

For the RPM-gated and DDG-retro reconstructions, the manufacturer's quiescent-period respiratory gating algorithm was used (Q.Static) with retention of approximately 50% of the data. As shown in Figure 1, this method retains data from the almost stationary period around the end of expiration while discarding data from the inspiration phase associated with most movement (*19*). For the DDG-retro reconstruction, the algorithm assesses the signal-to-noise ratio of respiratory frequencies within the waveform. This quality metric is defined as the R value of the waveform (*9*). The waveforms were also inspected and scored by a medical physicist similarly to a method used in our previous work (*9*). No threshold based on the R value (or visual score) was applied, with DDG applied to all datasets. The ungated-full reconstruction was included to compare the trade-off between applying respiratory motion correction that discards coincidences and applying no motion correction but with a similarly extended acquisition time.

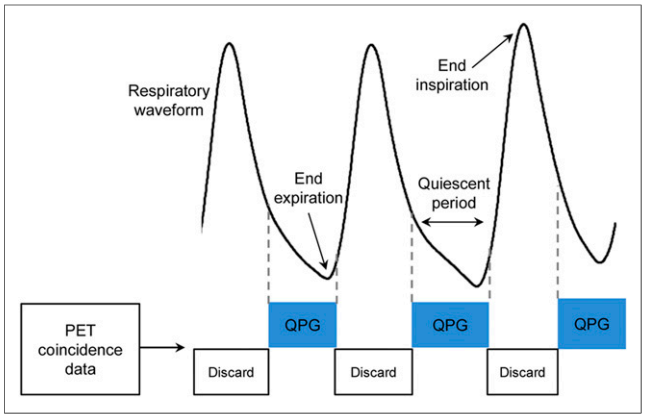

FIGURE 1. Depiction of quiescent period gating (QPG), in which part of respiratory cycle associated with relatively little motion is identified and retained in gated image.

Clinical Evaluation

Lesions in the region where respiratory gating was applied were identified by an experienced radiologist who was masked to the method of reconstruction and were used for assessment of SUV_{max}, SUV_{mean}, and lesion volume as determined using a threshold set at 40% of SUV_{max} (*16*). When the contrast between a lesion and the surrounding tissue was insufficient to determine lesion volume, only SUV_{max} was measured. This quantitative analysis was supplemented by a clinical evaluation performed by the radiologist, including a masked side-by-side comparison of the 4 images from each examination. Images were displayed in a random order and then scored (scale of 1–6) and ranked in terms of the overall diagnostic image quality. The image-quality scores were 1 (excellent, no or minimal heterogeneities), 2 (very good, subtle, tiny heterogeneities), 3 (good, small heterogeneities visible throughout), 4 (satisfactory, some significant heterogeneities of varying size and magnitude), 5 (numerous significant heterogeneities), and 6 (nondiagnostic). The noise in liver and bone marrow was also scored visually (scale of 1–6).

Statistical Analysis

To test for differences in the radiologist's clinical evaluation of image quality (ranks and scores) between the 4 groups, a Friedman test was performed. To test for differences in lesion uptake values and volume among the 4 groups, a 1-way ANOVA with repeated measures was used. Because of the nonnormal distribution of the lesion uptake values and volumes, these data were first transformed using the natural logarithm, after which they were approximately normal before application of the ANOVA. When significant differences among groups were indicated by the Friedman test, or by the ANOVA including a Greenhouse–Geisser correction for violation of sphericity as per the Mauchly test, these differences were assessed using a Wilcoxon signed-ranks test (for the ordinal data) or a paired *t* test (for the lesion uptake measures). For these post hoc tests, a Bonferroni adjustment was applied with consideration of 3 planned tests (DDG-retro compared with the other 3 datasets), resulting in a critical *P* value of 0.017. The presented *P* values are hence uncorrected for multiple comparisons but only considered significant if below 0.017. Statistical analyses were performed using SPSS, version 25.

RESULTS

Device and Algorithm Performance

If the external device failed to provide a gating signal, RPM-gated images either could not be reconstructed or had substantial,

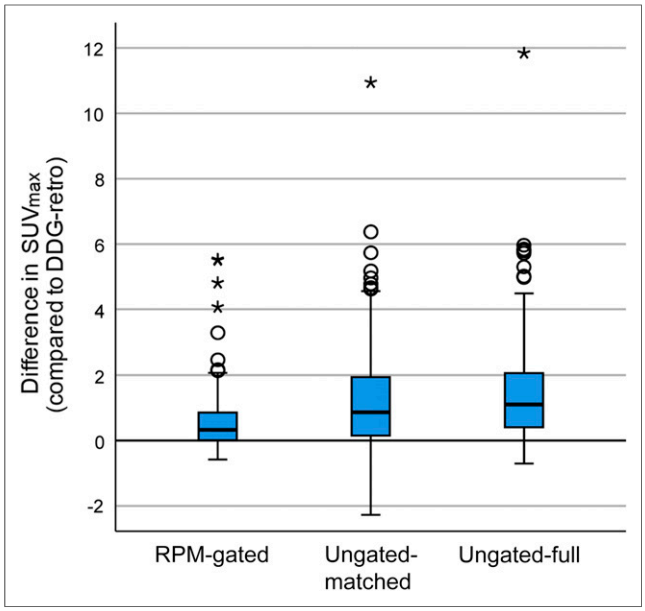

FIGURE 2. Box plots showing SUV_{max} for DDG-retro, minus that obtained from RPM-gated, ungated-matched, or ungated-full. Positive values indicate higher SUV_{max} in case of DDG-retro. Line on box indicates median.

obvious artifacts and were discarded. The external device failed to record a usable respiratory trace in 23 of the 144 PET/CT examinations (16%). From the 288 bed positions (144 examinations) to which DDG-retro was applied, the derived waveforms had a mean R value of 17.4 and a median value of 16.0. Of the 288 waveforms, 155 (54%) had R values greater than 15, which is the manufacturer's recommended threshold above which DDG-retro should be applied. The DDG-retro–derived waveforms were scored visually to be unsuitable for respiratory gating for 15 bed positions (from 13 examinations). The waveforms were, however, generated, and their use did not create image artifacts in the DDG-retro images. The external system failed in 3 of these 13 examinations. Of the 15 DDG-retro–derived waveforms considered unsuitable for gating, 4 had R values that were greater than 15, and 11 had R values that were less than 15. Eight of these 11 R values were particularly low ($R < 6$). According to this visual inspection, DDG-retro did not provide a robust respiratory trace for 5% of bed positions (15/288), as compared with RPM, which failed for 16% of examinations.

Lesion Quantification

Compared with each of the other reconstruction options, DDG-retro increased SUV_{max} and SUV_{mean} and decreased the threshold-defined lesion volume for this dataset. Paired differences in SUV_{max} are presented in Figure 2. The quantified uptake (SUV_{max}, SUV_{mean}) and lesion volumes significantly differed between groups in the 1-way, Greenhouse-Geisser–corrected ANOVA as applied to the logarithmically transformed data ($P < 0.0005$ for SUV_{max}; $P < 0.0005$ for SUV_{mean}; $P = 0.003$ for lesion volume). Paired t tests showed that the SUV results from DDG-retro were significantly higher than those for RPM-gated, ungated-matched, and ungated-full (Table 1). The differences between DDG-retro and RPM-gated were smaller than the differences between DDG-retro and ungated-matched or ungated-full.

Radiologist Scoring

From the 121 complete studies, the clinical evaluation revealed a significant difference in image quality (rank) among groups ($P < 0.0005$). The same was true for the scores assigned for overall image quality ($P < 0.0005$).

For most examinations, the same score and rank were assigned to RPM-gated and DDG-retro: equal ranks on 102 of 121 occasions (85%) and equal scores of overall image quality on 114 of 121 occasions (94%). DDG-retro was preferred (better rank) over RPM-gated in 16 examinations (13%), whereas in 3 examinations (2%) RPM-gated was preferred over DDG-retro. This occasional preference for DDG-retro over RPM-gated was statistically significant (Wilcoxon signed-ranks test; $P = 0.008$, $n = 121$). A similar result was obtained for comparison of the scores of overall image quality ($P = 0.008$).

Figure 3 shows the paired differences in scores of image quality. Of the 121 complete datasets, the top-ranked image was ungated-full

TABLE 1
Differences in Lesion Quantification Between DDG-Retro and the 3 Other Methods of Gating and Reconstruction

Parameter/DDG-retro with…	Lesions (*n*)	Difference (DDG-retro – other)		*P*
		Mean	25th, 75th percentiles	
SUV_{max}/RPM-gated	87	0.66 ± 0.1 g/mL	0.00, 0.87 g/mL	<0.0005
SUV_{max}/ungated-matched	107	1.3 ± 0.2 g/mL	0.06, 2.0 g/mL	<0.0005
SUV_{max}/ungated-full	107	1.6 ± 0.2 g/mL	0.38, 2.0 g/mL	<0.0005
SUV_{mean}/RPM-gated	54	0.44 ± 0.1 g/mL	−0.01, 0.60 g/mL	0.003
SUV_{mean}/ungated-matched	64	0.97 ± 0.2 g/mL	0.01, 1.60 g/mL	<0.0005
SUV_{mean}/ungated-full	64	1.2 ± 0.2 g/mL	0.36, 1.59 g/mL	<0.0005
Lesion volume/RPM-gated	54	−0.30 ± 0.1 cm^3	−0.52, 0.03 cm^3	0.009
Lesion volume/ungated-matched	64	−0.70 ± 0.2 cm^3	−0.98, −0.01 cm^3	0.005
Lesion volume/ungated-full	64	−0.83 ± 0.2 cm^3	−1.05, −0.03 cm^3	0.001

Data are mean differences (with SE on mean difference) and first and third quartiles, along with results from post hoc testing of transformed data. *P* values are uncorrected for multiple comparisons. Critical *P* value for statistical significance was 0.017 (lowered from 0.05 to allow for multiple comparisons).

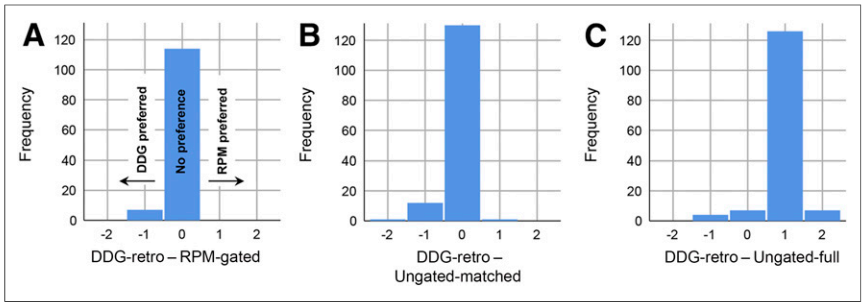

FIGURE 3. Comparison of clinical scoring between DDG-retro and RPM-gated (A), ungated-matched (B), and ungated-full (C). Lower score indicated preference, and hence negative scores represent preference for DDG-retro.

for 115 examinations; this was a significant preference over DDG-retro (Wilcoxon signed-ranks test; $P < 0.0005$, $n = 144$). Although the ungated-matched image was commonly ranked and scored equally with the respiratory gated images (equal rank to DDG-retro on 110 occasions; 76%), an overall preference for DDG-retro over ungated-matched was found to be statistically significant for ranks (Wilcoxon signed-ranks test; $P = 0.001$, $n = 144$) and image-quality scores ($P = 0.002$).

One or more lesions in the liver were identified in 23 of the 144 images. Considering this subset of data, DDG-retro was ranked superior to ungated-full in 6 of 23 (26%) cases. The overall preference for ungated-full was not statistically significant (Wilcoxon signed-ranks test; $P = 0.067$, $n = 23$). There was a trend for DDG-retro to be preferred over RPM-gated in this subset of data (preference for DDG-retro in 7 examinations, preference for RPM-gated in 2 examinations; $P = 0.083$, $n = 17$). DDG-retro was preferred over ungated-matched, with a better rank in 13 cases and with 8 ties ($P = 0.01$, $n = 23$). Paired differences in image quality for this dataset are presented in Figure 4. An example set of images is presented in Figure 5, with additional examples provided in Supplemental Figure 1 (supplemental materials are available at http://jnm.snmjournals.org).

Figure 6 provides an overview of the noise scores. Less noise was perceived in the ungated-full images (with 6 min of data) than in the other 3 image sets (each of which retained 3 min of data). These differences, observed for both the bone marrow and the liver noise scores, were significant (Wilcoxon signed-ranks test; $P < 0.0005$, $n = 143$). The differences among the 3 reconstructions that retained 3 min of data were comparatively small.

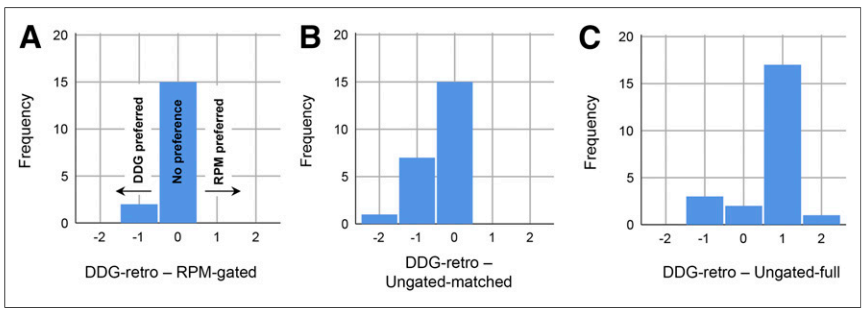

FIGURE 4. Considering only those studies with visible lesions in liver, comparison of clinical scoring between DDG-retro and RPM-gated (A), ungated-matched (B), and ungated-full (C). Lower score indicated preference, and hence negative scores represent preference for DDG-retro.

DISCUSSION

This study found a commercially developed data-driven respiratory gating algorithm to provide superior respiratory gating of PET data, as compared with gating using an external device in the setting of clinical ^{18}F-FDG PET/CT imaging. This superiority was demonstrated by a larger increase in SUV_{max} on application of the respiratory gating, accompanied by improved clinical image quality. In 85% of cases, the 2 methods of gating were considered to give images of equal quality when scored by a single, experienced radiologist, but with an occasional (13%) preference for DDG-retro over RPM. Furthermore, DDG-retro had a lower failure rate; 100% of the DDG-retro images were considered to be clinically acceptable. For the 13 of 144 examinations in which the DDG-retro could not extract a suitable respiratory waveform, this inability did not prevent reconstruction of the PET images and did not introduce image artifacts. In the 23 of 144 (16%) examinations in which the external device failed, this failure produced errors in workflow or introduced low-count image artifacts due to missing respiratory triggers.

The study also indicates that quiescent-period gating, with 50% of coincidences discarded, rarely provides an image quality superior to that provided by no gating with retention of all coincidences. The radiologist ranked DDG-retro as better than ungated-full in just 9 of 144 examinations (with no ties). Quiescent-period gating (from a 6-min acquisition) fared better than no gating but from a shorter (3-min) acquisition, with the gated images generally equivalent (tied rank, 110/144 examinations; 76%) or preferred (superior rank, 26/144 examinations; 18%). The preference for gated images over ungated-full occurred only when disease was present in the abdominal organs, in which case there was a preference for gated images 26% of the time (superior rank, 6/23 examinations). This occasional visual preference was accompanied by increased contrast (reduced respiratory blurring) in the PET images on application of the gating, as evidenced by an increase in SUV_{max} and SUV_{mean}, with a concurrent decrease in the threshold-defined lesion volume.

The primary measure under investigation in the study was SUV_{max}, chosen to remove subjectivity from the comparison. A radiologist assisted in the identification of lesions but also provided clinical scoring, which is expected to suffer from a bias toward a smoother image when there are no obvious abdominal lesions. There is a preference for this smoother image in this region because the reduced noise leads to greater confidence about a lack of abnormality (such as small-volume disease). Such an image may, however, be less optimal for diagnostic purposes, as demonstrated by the occasional visualization—on the respiratory gated images—of a liver lesion that is absent from the nongated, full-count image (Fig. 5); in these specific cases, it is of no surprise that the respiratory gated image received a superior score. The rate at which respiratory gated imaging is preferred is then dependent on the

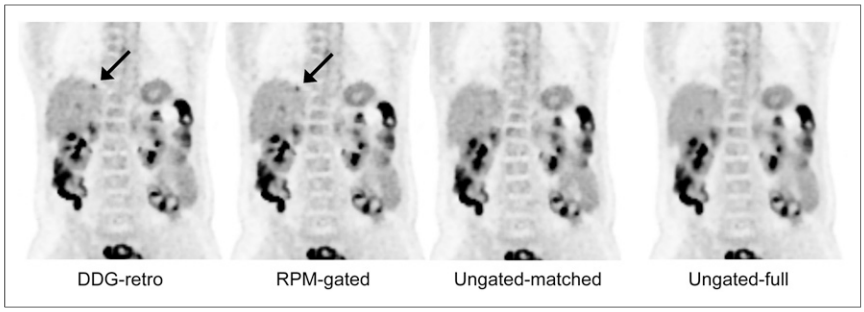

FIGURE 5. Coronal slices showing ^{18}F-FDG–avid liver metastasis (indicated by arrows) that is easier to detect and has higher SUV_{max} on 2 gated reconstructions than without gating. In this example, DDG-retro and RPM-gated images received equal score for overall image quality, and both were considered superior to ungated images. Lesion indicated by arrow was not considered to be definitely visible on ungated-matched image and was borderline-visible on ungated-full image. One can also see reduction in noise in ungated-full image, as compared with other 3 images. Images are on SUV grayscale of 0–6.

rate at which difficult-to-detect abdominal lesions are present in the patient population. Two important ramifications for patient care should be considered from these results: small abdominal lesions were generally clearer on gated images, and hence, respiratory gating has the potential to alter patient pathways (if gating is required for metastatic disease to be detected); SUV_{max} was usually increased by respiratory gating and is likely more accurate; hence, gating needs to be applied consistently in any disease-monitoring investigations and in the definition of treatment thresholds based on SUV_{max}. In the current study, we applied gating to all patients rather than preselecting a subgroup of patients based on disease location or the amplitude of their respiratory motions.

The preference for DDG-retro over RPM-gated was likely a result of 2 factors. First, the respiratory waveform derived from motion information contained in the PET data should be more representative of the motion of abdominal organs than is tracking of motion of the chest wall. Second, the data-driven technique determined the respiratory triggers after extraction of the whole respiratory waveform, as opposed to using a prospective triggering algorithm to insert respiratory triggers into the data stream during acquisition.

A limitation of this study is its retrospective nature, together with the retrospective application of DDG without any R-threshold to 2 preselected bed positions. Although the same DDG algorithm is used in MotionFree, we used the term *DDG-retro* to distinguish that we did not use the real-time R-threshold based application of DDG that is available within the MotionFree product (2019 release). The use of an R threshold would reduce the failure rate for DDG and is likely to assist in the selection of those specific patients (and bed positions) for which respiratory gating will be of benefit. There may have been bed positions more superior or inferior than the preselected ones that would have benefitted from respiratory gating. For the Bayesian penalized-likelihood image reconstruction, a fixed β-value of 400 was used for all 4 reconstructions and all bed positions; this value may be suboptimal for the 6-min bed positions in the ungated-full reconstructions. We did not attempt to compare the commercially developed DDG algorithm with the other approaches to DDG (*15,16*). For a detailed discussion of such methods, the reader is referred to previous publications (*6,9,20*).

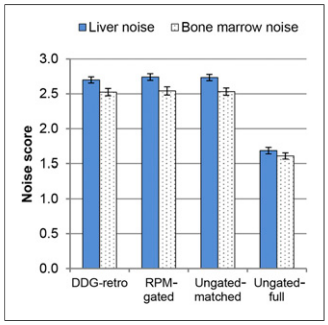

FIGURE 6. Comparison of noise scoring across 4 image reconstructions. Error bars represent SEs on mean.

Furthermore, in this study there was no attempt to improve the alignment of the free-breathing CT image with the quiescent-phase PET image. Although images from the 2 modalities were often closely aligned, there were occasions on which the CT exposure occurred at a different respiratory phase, leading to misalignment of the images and the introduction of well-recognized attenuation-correction and scatter-correction artifacts. Application of quiescent-period gating in such a manner is known to cause changes in the magnitude of these artifacts, with corresponding changes in lesion quantification (*21*). Although these changes do not confound our comparison of DDG-retro and RPM-gated images (as both make use of the same CT attenuation correction and a similar respiratory phase for the PET data), they are a confounding factor for comparison of gated images and nongated images, and hence, the quantitative comparison we performed is subject to this caveat. A robust method to realign free-breathing CT datasets to those from respiratory gated PET could increase the benefits of respiratory gated PET imaging in the future.

Similarly, this study considered only quiescent-period gating, as we primarily sought to compare device-based and deviceless respiratory gating. Several manufacturers offer quiescent-period gating, with different methods for identifying the part of the waveform to retain and with user-defined parameters to provide different retention fractions (e.g., 25%–50%) (*19,22*). PET respiratory gating with retention of more than 50% of coincidences has been previously described (*23,24*), but the current methods are complex and rarely used in practice. Additional methods that retain a higher fraction of the coincidences are under development. This study suggests that retention of more than 50% of coincidences may be required before respiratory gated PET imaging can routinely and unequivocally outperform ungated PET imaging.

CONCLUSION

In the context of oncologic ^{18}F-FDG PET/CT imaging, a commercially developed, data-driven respiratory gating technique provided performance superior to that of a commercially available, external-device–based respiratory gating system. The data-driven method is likely to increase the use of respiratory gating in clinical PET imaging because of superior performance and improved workflow.

DISCLOSURE

Oxford University Hospitals NHS Foundation Trust has a research contract with GE Healthcare covering loan of equipment but without financial support. Daniel McGowan is funded by an NIHR/HEE Clinical Lectureship. This paper presents independent

research funded by the NIHR and HEE. The views expressed are those of the authors and not necessarily those of the NHS, the NIHR, HEE, or the Department of Health. No other potential conflict of interest relevant to this article was reported.

KEY POINTS

QUESTION: How does DDG for ^{18}F-FDG PET/CT perform in comparison to device-based respiratory gating?

PERTINENT FINDINGS: A masked comparison of 144 ^{18}F-FDG PET/CT images found a significant preference for DDG over the device-based system, despite similar scores of image quality and similar quantification of lesions in most patients.

IMPLICATIONS FOR PATIENT CARE: DDG is likely to increase the use of respiratory gating in clinical PET, leading to fewer respiratory artifacts and potentially increasing diagnostic accuracy.

REFERENCES

1. Clifford MA, Banovac F, Levy E, Cleary K. Assessment of hepatic motion secondary to respiration for computer assisted interventions. *Comput Aided Surg.* 2002;7:291–299.
2. Bussels B, Goethals L, Feron M, et al. Respiration-induced movement of the upper abdominal organs: a pitfall for the three-dimensional conformal radiation treatment of pancreatic cancer. *Radiother Oncol.* 2003;68:69–74.
3. van der Vos CS, Koopman D, Rijnsdorp S, et al. Quantification, improvement, and harmonization of small lesion detection with state-of-the-art PET. *Eur J Nucl Med Mol Imaging.* 2017;44:4–16.
4. Pépin A, Daouk J, Bailly P, Hapdey S, Meyer M-E. Management of respiratory motion in PET/computed tomography: the state of the art. *Nucl Med Commun.* 2014;35:113–122.
5. Thielemans K, Rathore S, Engbrant F, Razifar P. Device-less gating for PET/CT using PCA. In: *2011 IEEE Nuclear Science Symposium Conference Record. Piscataway,* NJ: IEEE; 2011:3904–3910.
6. Thielemans K, Schleyer P, Marsden PK, Manjeshwar RM, Wollenweber SD, Ganin A. Comparison of different methods for data-driven respiratory gating of PET data. In: *2013 IEEE Nuclear Science Symposium and Medical Imaging Conference (2013 NSS/MIC). Piscataway,* NJ: IEEE; 2013:1–4.
7. Bertolli O, Arridge S, Wollenweber SD, Stearns CW, Hutton BF, Thielemans K. Sign determination methods for the respiratory signal in data-driven PET gating. *Phys Med Biol.* 2017;62:3204–3220.
8. Walker MD, Bradley KM, McGowan DR. Evaluation of principal component analysis-based data-driven respiratory gating for positron emission tomography. *Br J Radiol.* 2018;91:20170793.
9. Walker MD, Morgan AJ, Bradley KM, McGowan DR. Evaluation of data-driven respiratory gating waveforms for clinical PET imaging. *EJNMMI Res.* 2019;9:1.
10. Morley NCD, McGowan DR, Gleeson FV, Bradley KM. Software respiratory gating of positron emission tomography–computed tomography improves pulmonary nodule detection. *Am J Respir Crit Care Med.* 2017;195:261–262.
11. Rietzel E, Chen GTY, Choi NC, Willet CG. Four-dimensional image-based treatment planning: target volume segmentation and dose calculation in the presence of respiratory motion. *Int J Radiat Oncol Biol Phys.* 2005;61:1535–1550.
12. Hoisak JDP, Sixel KE, Tirona R, Cheung PCF, Pignol J-P. Correlation of lung tumor motion with external surrogate indicators of respiration. *Int J Radiat Oncol Biol Phys.* 2004;60:1298–1306.
13. Li R, Mok E, Han B, Koong A, Xing L. Evaluation of the geometric accuracy of surrogate-based gated VMAT using intrafraction kilovoltage x-ray images. *Med Phys.* 2012;39:2686–2693.
14. Büther F, Jones J, Seifert R, Stegger L, Schleyer P, Schäfers M. Clinical evaluation of a data-driven respiratory gating algorithm for whole-body positron emission tomography with continuous bed motion. *J Nucl Med.* February 14, 2020 [Epub ahead of print].
15. Kesner AL, Chung JH, Lind KE, et al. Validation of software gating: a practical technology for respiratory motion correction in PET. *Radiology.* 2016;281:239–248.
16. Büther F, Vehren T, Schäfers KP, Schäfers M. Impact of data-driven respiratory gating in clinical PET. *Radiology.* 2016;281:229–238.
17. Bettinardi V, Presotto L, Rapisarda E, Picchio M, Gianolli L, Gilardi MC. Physical performance of the new hybrid PET/CT Discovery-690. *Med Phys.* 2011;38:5394–5411.
18. Teoh EJ, McGowan DR, Macpherson RE, Bradley KM, Gleeson FV. Phantom and clinical evaluation of the Bayesian penalized likelihood reconstruction algorithm Q.Clear on an LYSO PET/CT system. *J Nucl Med.* 2015;56:1447–1452.
19. Liu C, Alessio A, Pierce L, et al. Quiescent period respiratory gating for PET/CT. *Med Phys.* 2010;37:5037–5043.
20. Kesner AL, Kuntner C. A new fast and fully automated software based algorithm for extracting respiratory signal from raw PET data and its comparison to other methods. *Med Phys.* 2010;37:5550–5559.
21. Meier JG, Einstein SA, Diab RH, Erasmus LJ, Xu G, Mawlawi OR. Impact of free-breathing CT on quantitative measurements of static and quiescent period-gated PET Images. *Phys Med Biol.* 2019;64:105013.
22. van Elmpt W, Hamill J, Jones J, De Ruysscher D, Lambin P, Ollers M. Optimal gating compared to 3D and 4D PET reconstruction for characterization of lung tumours. *Eur J Nucl Med Mol Imaging.* 2011;38:843–855.
23. Huang T-C, Chou K-T, Wang Y-C, Zhang G. Motion freeze for respiration motion correction in PET/CT: a preliminary investigation with lung cancer patient data. *BioMed Res Int.* 2014:167491.
24. Hong I, Jones J, Hamill J, Michel C, Casey M. Elastic motion correction for continuous bed motion whole-body PET/CT. In: *2016 IEEE Nuclear Science Symposium, Medical Imaging Conference and Room-Temperature Semiconductor Detector Workshop (NSS/MIC/RTSD). Piscataway,* NJ: IEEE; 2016:1–2.